

Thermal and magnetic phase transition properties of a binary alloy spherical nanoparticle: A Monte Carlo simulation study

Z.D. Vatansever*, E. Vatansever

Department of Physics, Dokuz Eylül University, Tr-35160 İzmir, Turkey

Abstract

We have used the Monte Carlo (MC) simulation method with Metropolis algorithm to study the finite temperature phase transition properties of a binary alloy spherical nanoparticle with radius r of the type $A_p B_{1-p}$. The system consists of two different species of magnetic components, namely, A and B , and the components of the system have been selected A and B to be as $\sigma = 1/2$ and $S = 1$, respectively. A complete picture of phase diagrams, total magnetizations and susceptibilities in related planes have been presented, and the main roles of the radius of nanoparticle, active concentration value of type- A atoms as well as other system parameters on the thermal and magnetic phase transition features of the considered system have been discussed in detail. Our MC investigations clearly show that it is possible to control the critical characteristic behaviors of the system with the help of adjustable Hamiltonian parameters.

Keywords: Binary alloy systems, magnetic nanoparticles, Monte Carlo simulation.

1. Introduction

When the physical size of a magnetic system is reduced to a characteristic length, the system has a bigger surface area to volume ratio giving rise to a great many unusual thermal and magnetic properties different from the conventional bulk systems [1]. In recent years, there has been active research on small-size nanoparticles both experimentally and theoretically because of their technological [2, 3, 4] and biomedical applications [5, 6, 7, 8, 9]. For example, from the experimental point of view, the multi-functionality nanowires with an iron core and an iron oxide shell have been synthesized by a facile low-cost fabrication process in Ref. [9]. Here, Ivanov and co-workers report that a multi-domain state at remanence can be obtained, which is an attractive feature for the biomedical applications. Magnetic proximity effect in ferrimagnetic/ferromagnetic core/shell Prussian blue analogues molecular magnet has been found by Bhatt and co-workers in Ref. [10]. They synthesize a ferrimagnetic core of $\text{Mn}_{1.5}[\text{Cr}(\text{CN})_6] \cdot 7.5\text{H}_2\text{O}$ surrounded by a ferromagnetic shell of $\text{Ni}_{1.5}[\text{Cr}(\text{CN})_6] \cdot 7.5\text{H}_2\text{O}$, and note that such a process allows us to enhance the critical temperature of the core/shell nanoparticle system, compared to the bare-core and bare-shell critical temperatures.

On the other hand, from the theoretical point of view, a great deal of studies have been devoted to investigate the thermal and magnetic features of nanoparticles such as nanocube, nanosphere, nanorod, nanotube as well as nanowire by means of several types of methods such as mean-field theory (MFT) [11, 12, 13], Green function formalism (GF) [14], cluster variation method (CVM) [15], effective-field theory (EFT) with single-site correlations [16, 17, 18, 19, 20, 21, 22], and MC simulation technique [11, 23, 24, 25, 26, 27, 28, 29, 30, 31, 32, 33]. For example, by making use of MC simulation technique with Metropolis algorithm, thermal and magnetic phase transition properties of antiferromagnetic/ferrimagnetic core/shell nanoparticles have been studied by Vasilakaki and co-workers in detail [25]. It has been reported that the coercivity and loop shift show a non-monotonic dependence with the core diameter and shell thickness, in agreement with the experimental data. Magnetic phase transitions as well as hysteretic features of a graphyne core/shell nanoparticles have been investigated in Ref. [26] based on MC simulation method. It has been found that the considered system exhibits a number of unusual and characteristic treatments such as the occurrence

*Corresponding author. Tel.: +90 3019531; fax: +90 2324534188.
 Email address: zeynep.demir@deu.edu.tr (Z.D. Vatansever)

of one and two compensation temperatures. Moreover, magnetic phase transition properties of a single spherical core/shell nanoparticle, consisting of a ferromagnetic core surrounded by a ferromagnetic shell with antiferromagnetic interface coupling have been realized within the framework of MC simulation scheme [27]. It is underlined that for appropriate values of the system parameters, multiple compensation points may emerge in the system. They also analyzed the core radius and shell thickness dependencies of the critical behavior of the system, and they found that the values of compensation and critical temperatures vary with changing value of the particle size, and they reach saturation values for high values of the particle size.

Furthermore, determination of equilibrium phase transition properties of binary alloy systems containing disorder effects problems which may be arisen from a random distributions of the magnetic components or random exchange interactions between the magnetic components in the material has a long history. Many studies have been performed regarding the physical properties of disordered binary magnetic materials with quenched randomness where the random variables of a system may not change its value over time based on a variety of techniques such as MFT [34, 35, 36, 37], EFT [38, 39, 40, 41, 42] as well as MC [43, 44, 45, 46], in the context of bulk materials. We learned from these works quenched disordered binary alloy systems with different signs and unequal magnitudes of the spin-spin interactions and single ion-anisotropy exhibit unusual and interesting thermal and magnetic behaviors such as presence of a reentrant type character in the magnetization versus temperature profile, compensation and also spin-glass behaviors. Keeping the discussions mentioned above in mind, we intend to elucidate the finite temperature phase transitions and critical properties of a binary alloy spherical nanoparticle with radius r of the type A_pB_{1-p} in this study. The system consists of two different species of magnetic spin components, i.e., A and B , and we select the components of the system A and B to be as $\sigma = 1/2$ and $S = 1$, respectively. In the system, there aren't any un-occupied lattice sites and each lattice site is occupied by type- A or $-B$ atom, depending on the active concentration value of type- A components, p . We perform MC simulation, using Metropolis algorithm and determine the effects of the p , radius of spherical nanoparticle as well as other system parameters on the phase transition features of the considered system. To the best of our knowledge, there are no works regarding the thermal phase transition properties of binary alloy type spherical nanoparticle systems, except from Ref. [29] where compensation behavior of a ferrimagnetic spherical nanoparticle system with binary alloy shell is studied by means of MC simulation method. It has been stated that the system exhibits one, two or even three compensation points, depending on the system parameters. We should note that our model is completely different from the system studied in Ref. [29]. That is to say, the magnetic components A and B can locate any place of the nanoparticle, whereas they can only locate the shell part of the particle, in the mentioned work.

The plan of the remainder parts of the paper is as follows: In section 2, we present our model. The results and discussions are given in section 3, and finally section 4 contains our conclusions.

2. Formulation

We consider a binary alloy spherical nanoparticle system of the type A_pB_{1-p} with total radius r , which is schematically shown in figure 1. The lattice sites are randomly occupied by two different species of magnetic components A and B with the concentration p and $1 - p$, respectively. The Hamiltonian describing our model of magnetic system is given by:

$$\hat{H} = -J \sum_{\langle i,j \rangle} [\delta_{iA}\delta_{jA}\sigma_i\sigma_j + \delta_{iB}\delta_{jB}S_iS_j + \delta_{iA}\delta_{jB}\sigma_iS_j + \delta_{iB}\delta_{jA}S_i\sigma_j] - \Delta \sum_i \delta_{iB}S_i^2, \quad (1)$$

here $J > 0$ denotes the ferromagnetic spin-spin interaction term between nearest neighbor spins while Δ refers to the single-ion anisotropy term. The σ and S are classic Ising spin variables which can take values of $\sigma = \pm 1/2$ and $S = \pm 1, 0$ for the magnetic components- A and $-B$ of system, respectively. The symbol $\delta_{i\alpha} = 1$ ($\alpha = A$ or B) if site i is occupied by type- α atom and 0 otherwise. The first summation in Eq. (1) is over the nearest neighbor pairs while the second one is over all lattice sites occupied by type- B atoms.

In order to investigate the thermal and magnetic phase transition properties of the binary alloy type spherical nanoparticle system, we use the MC simulation technique with local spin update Metropolis algorithm [47, 48]. We simulate the system with radius r up to 18, located on a simple cubic lattice, under free boundary conditions applied in all directions. We can summarize the simulation procedure as follows. First, the simulation starts at a high temperature value using random initial condition, and then the system is slowly cooled down with a reduced

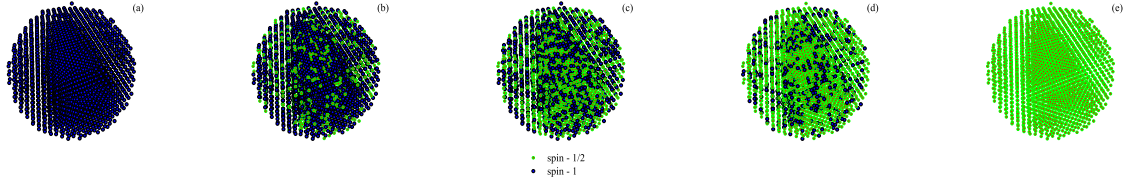


Figure 1: (Color online) Schematic representations of the binary alloy spherical nanoparticle of the type A_pB_{1-p} for five selected active concentration values of magnetic components, namely (a) $p = 0$, (b) $p = 0.25$, (c) $p = 0.5$, (d) $p = 0.75$ and (e) $p = 1$.

temperature step $k_B\Delta T/J = 2 \times 10^{-2}$, where k_B and T are Boltzmann constant and absolute temperature, respectively. The spin configurations are generated by selecting the sites sequentially through the binary alloy type nanoparticle system, and making single-spin flip attempts, which are accepted/rejected according to the Metropolis algorithm. Thermal variations of various thermodynamic quantities are generated over 50 independent computer experiments. In each computer experiment, the first 10^4 MC steps have been discarded for thermalization process, and the numerical data are collected over the next 4×10^4 MC steps. Based on our test investigations, we note that this amount of transient steps are found to be sufficient for thermalization for the whole range of the parameter sets.

Our program calculates the the instantaneous values of the magnetizations as follows:

$$M_A = \frac{1}{N_A} \sum_{i=1}^{N_A} \sigma_i, \quad M_B = \frac{1}{N_B} \sum_{i=1}^{N_B} S_i, \quad M_T = \frac{N_A M_A + N_B M_B}{N_A + N_B} \quad (2)$$

where N_A and N_B correspond to the total number of ions A and B in the system, respectively. In order to determine the magnetic phase transition point separating the ordered and disordered phases from each other, we use and check the thermal variation of the total susceptibility, which is defined by:

$$\chi_T = (N_A + N_B) \frac{(\langle M_T^2 \rangle - \langle M_T \rangle^2)}{k_B T}. \quad (3)$$

3. Results and Discussion

In this section, we present our MC simulation results of a binary alloy nanoparticle with a spherical shape. We discuss the magnetic properties and critical behaviour of the system by analysing the phase diagrams in various planes.

Firstly, we investigate the dependence of the transition temperature from ferromagnetic to paramagnetic phase of the binary alloy nanoparticle on the concentration of spin-1/2 atoms in the absence of crystal-field interaction. Figure 2(a) shows the phase-diagram of the system in $(p - k_B T_C/J)$ plane for six selected values of nanoparticle radius $r = 4, 6, 8, 10, 12$ and 14 . From the figure one can observe that for all the values of nanoparticle radius under consideration, as the number of type- A atoms is increased starting from $p = 0$ to 1, the transition point moves to a lower value in the temperature axis and thereby ordered regions in $(p - k_B T_C/J)$ becomes narrower. This is due to the fact that when one increases p , the energy contribution coming from the exchange interaction term becomes smaller and consequently the system exhibits phase transition at lower temperature values.

A second point which should be noted about Figure 2(a) is the variation of the phase diagram separating the spin-ordered and disordered phases with the size of the nanoparticle. It is obvious that when the radius of the nanoparticle begins to rise the critical temperature of the system starts to shift to higher temperature values for all p . This can be observed explicitly from Figure 2(b) and 2(c) where the total magnetization M_T and susceptibility χ_T of the system are depicted as a function of the temperature with varying particle radius for $p = 0.5$. It is seen that the total magnetization of the system gradually decreases starting from its saturation value of $M_T = 0.75$ with increasing thermal agitation, and it vanishes continuously at different critical temperature values depending on the considered value of nanoparticle size. As seen from the Figure 2(c), the susceptibility curves demonstrate a smooth cusp for smaller binary alloy spherical nanoparticles. When the radius of the nanoparticle increases, a divergent treatment emerges in the susceptibility curve at the phase transition point which indicates of a second-order phase transition. In addition, the position of the

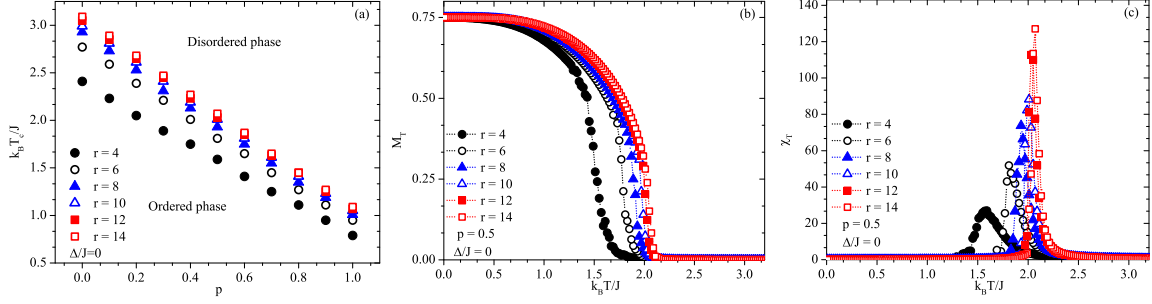


Figure 2: (Color online) (a) Magnetic phase diagrams in the $(p - k_B T_C / J)$ plane of the binary alloy spherical nanoparticle system. The curves are presented for various values of radius of the spherical nanoparticle, $r = 4, 6, 8, 10, 12$ and 14 . Effects of the radius on the thermal dependencies of total (b) magnetization M_T and (c) susceptibility χ_T of the system for $p = 0.5$. All figures are obtained for value of $\Delta/J = 0$.

susceptibility peak moves to higher temperature region with increasing nanoparticle radius. It should be emphasized here that our numerical findings regarding the thermal and phase transition properties of the present system are in accordance with the recently published works where equilibrium and non-equilibrium phase transition features of different types of binary alloy systems [45, 46] as well as a clean nanowire with radius r and length L under the influence of a time dependent magnetic field have been implemented by utilizing MC simulation technique [49].

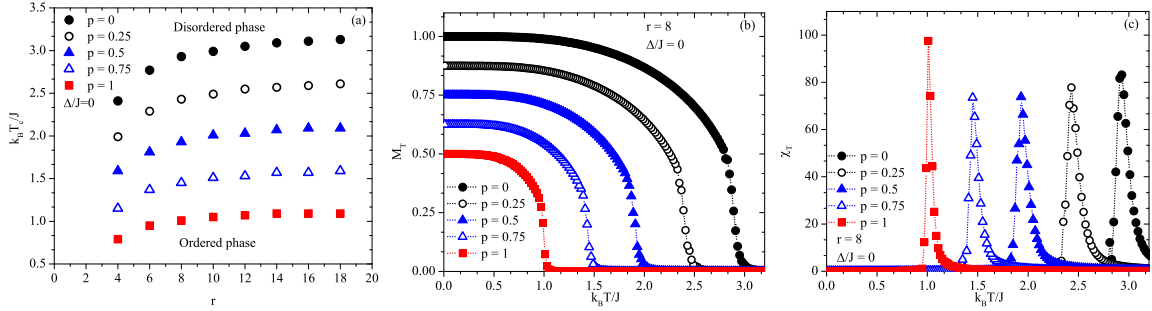


Figure 3: (Color online) Radius dependency of the critical point of binary alloy spherical nanoparticle system for considered values of active concentrations of type-A atoms such as $p = 0, 0.25, 0.5, 0.75$ and 1 . Influences of the active concentration of type-A atoms on the temperature dependencies of total (b) magnetizations M_T and (c) susceptibility χ_T of the system with $r = 8$ corresponding to the Figure 3(a). All figures are displayed for value of $\Delta/J = 0$.

Next, we examine the change of the transition temperature from ordered to disordered phase with the nanoparticle radius r . Figure 3(a) shows the critical temperature as a function of the nanoparticle radius for different values of the concentration of type-A atoms in the system in the case of $\Delta/J = 0$. Due to the high surface to volume ratio for small size particle, and the lower coordination number of the surface atoms, the phase transition temperature of the system decreases with the reduction of its size. This fact is evidently seen in Figure 3(a). As the size of the system is increased starting from $r = 4$, the phase transition temperature moves to higher temperature value. The reason is that when the size of the nanoparticle becomes larger, the energy contribution from the spin-spin interaction term increases and thus more thermal energy is required for occurrence of a phase transition. As one further rises r , the critical temperature becomes nearly independent of the particle-size, where surface effects may be negligible, and it saturates at a certain temperature value which sensitively depends on the concentration of type-A atoms. We show the thermal dependencies of the total magnetization and susceptibility curves for several values of concentration of type-A atoms and a fixed value of radius $r = 8$ of particle in Figure 3(b) and 3(c) corresponding to the Figure 3(a), respectively. The behaviour of the total magnetization of the binary alloy nanoparticle system exhibits a second-order phase transition at different critical temperature values depending on p . Also the positions of the peaks of the susceptibility curves support the magnetization data and shift to lower temperature region with increasing p . It should be pointed out that melting temperature dependencies of the various types of binary alloy nanoparticle, for example

$\text{In}_{0.3}\text{Sn}_{0.7}$, CuNi and $\text{Cu}_{0.25}\text{Ni}_{0.75}$ have been discussed in Ref. [50], in the context of size and composition of binary nanoparticles.

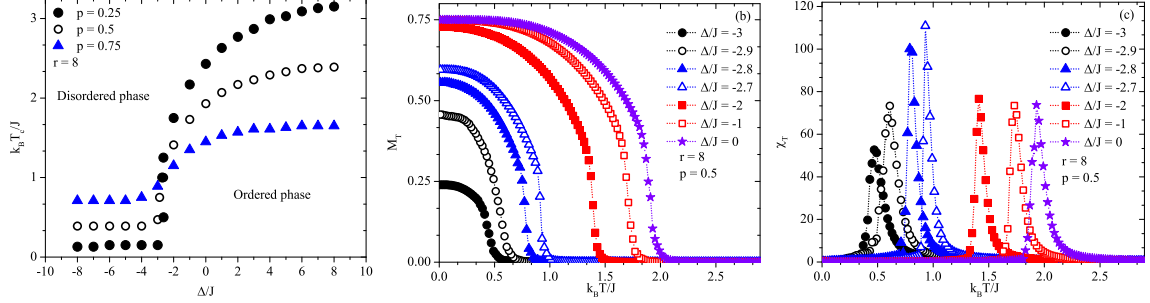


Figure 4: (Color online) Magnetic phase diagrams in $(\Delta/J - k_B T_C/J)$ plane of the binary alloy spherical nanoparticle system, which are shown for different values of the active concentrations of type- A atoms such as $p = 0.25, 0.5$ and 0.75 . Influences of the single-ion anisotropies on the temperature dependencies of the total (b) magnetizations M_T and (c) susceptibility χ_T of the system with selected value of $p = 0.5$. All figures are presented for value of radius $r = 8$.

In the following analysis, we study the effects of the single-ion anisotropy term on the ferromagnetic to paramagnetic transition temperature of the binary alloy nanoparticle system. In Figure 4(a), the phase boundary curve in $(\Delta/J - k_B T_C/J)$ space in the case of three selected values of concentration of type- A atoms, $p = 0.25, 0.5$ and 0.75 , is presented for a nanoparticle radius of $r = 8$. As one can see clearly from the figure that in the case of low-negative and high-positive single-ion anisotropy region, the phase transition points saturate at particular temperature values. This saturation temperature strongly depends on the concentration of spin-1/2 atoms. In the high-positive Δ/J region, as one increases the number of A atoms in the system, the saturation occurs at low temperature values. This is due to the fact that replacing the spin-1 atoms with spin-1/2 atoms in the system (increasing p) means decreasing the number of atoms under the influence of single-ion anisotropy term and this causes the system to exhibit phase-transition at relatively low temperatures. Conversely, for large negative Δ/J values, increasing p results in saturation at high temperature values. Apart from these, in small single-ion anisotropy region, critical temperature rises when the amount of Δ/J is increased. Thermal variations of the total magnetization and the corresponding magnetic susceptibility for the binary alloy spherical nanoparticle system for several negative values of single-ion anisotropy terms and with a fixed concentration value $p = 0.5$ and nanoparticle radius $r = 8$ are shown in Figure 4(b) and 4(c), respectively. For the present investigation, since the positive values of the Δ/J terms are no significant effects on the magnetization profiles, except from its critical temperature, we are restricted ourselves to the relatively low and high negative Δ/J values. As it is seen from Figure 4(b) that the saturation value of the total magnetization is $M_T = 0.75$ when $\Delta/J = 0$. However, because of the single-ion anisotropy term acting on B -type atoms, as value of single-ion anisotropy decreases, the saturation value of the total magnetization also decreases from $M_T = 0.75$. Besides, the susceptibility peaks appear at lower values of the temperature axis when the single-ion anisotropy term becomes more negative. It should be underlined that we have not observed a behavior indicating a first-order phase transition for all the selected values of p and single-ion anisotropy term.

Finally, we clarify the variations of the magnetic phase diagram in $(\Delta/J - k_B T_C/J)$ space with the size of the nanoparticle. Figure 5(a) reveals the critical temperature versus reduced single-ion anisotropy term for several values of nanoparticle radius, $r = 4, 6, 8, 10, 12$ and 14 . It is possible to deduce from the figure that the behavior of phase separation curve between ferromagnetic and paramagnetic phases is similar for each value of r . One of the main differences is that saturation value of the critical temperature takes larger values with increasing particle size for all Δ/J . In figure 5(b) and 5(c), we give the temperature dependent of total magnetization and susceptibility profiles of the system for several values of nanoparticle radius with $p = 0.5$ and $\Delta/J = -2$, respectively. We note that the saturation value of the total magnetization alters very little with varying nanoparticle radius and becomes zero at different critical temperature values which can be clearly seen from the positions of maximum values of the magnetic susceptibility versus temperature curves.

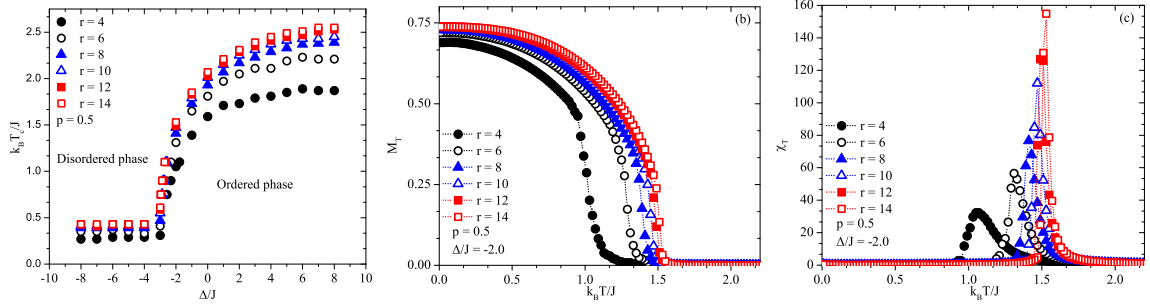


Figure 5: (Color online) Effects of the varying values of radius of the binary alloy spherical nanoparticle on the magnetic phase diagrams displayed in $(\Delta/J - k_B T_C/J)$ plane. Variations of the total (b) magnetizations M_T and (c) susceptibility χ_T as a function of the temperature for several values of radius of the system with $\Delta/J = -2$. The curves are presented for a selected value of active concentration of type-A atoms, $p = 0.5$.

4. Conclusions

In this paper, we have considered the finite temperature phase transition features of a binary alloy spherical nanoparticle with radius r of the type $A_p B_{1-p}$. For this purpose, we use MC simulation method with single-site update Metropolis algorithm. As a binary alloy spherical nanoparticle, we select a system consisting of spin-1/2 and spin-1 magnetic components. They are randomly distributed depending on the selected value of the active concentration of type-A atoms. It is obvious that the cases of $p = 1$ and 0 correspond to the clean Ising and Blume-Capel spherical nanoparticles, respectively. For both two values of p mentioned above, there is no lattice site containing disorder arising from the existence of different species of magnetic components. However, the considered system composes of randomly located spin-1/2 and spin-1 components, except from these two values of p . Our findings clearly indicate that it is possible to control the thermal and magnetic phase transition properties of the system with the help of adjustable extrinsic parameters p and r as well as other intrinsic system parameters. The most important observations found in the present work can be shortly summarized as follows:

- For a fixed value of r and value of $\Delta/J = 0$, our results suggest that magnetic phase transition point of the system prominently decreases when the value of active concentration of type-A atoms increases starting from zero. One can see that phase transition curves given in $(p - k_B T_C/J)$ plane exhibit an almost linear character, for all considered values of r . It should be underlined that concentration dependencies of the critical temperatures of a binary alloy bulk system driven by a time dependent magnetic field have been discussed in Ref. [51] by means of MC simulation method. If one compares the figure 2 of Ref. [51] with figure 2 of the present study, one can easily see the similarities and differences between the two systems.
- For a fixed value of p and value of $\Delta/J = 0$, it is found that when the radius of the spherical nanoparticle increases starting from $r = 4$, the critical temperature begins to shift to higher temperature regions. If the r further increases, and reaches a certain value which strongly depends on the Hamiltonian parameters, the phase transition point saturates a characteristic value.
- Moreover, thermal and magnetic phase transition features of the system sensitively depends on the single-ion anisotropy term. Both large negative and positive values of Δ/J term give rise to saturation of the critical temperature of the system to a characteristic value. It is worth to note that such type of observation originating from the existence of single-ion anisotropy has been found in Ref. [52]. Here, dynamic phase transition properties of a binary alloy ferromagnetic alloy under the presence of a time dependent magnetic field have been analyzed for a two dimensional square lattice.

Finally, we notice that it could be interesting to focus on the effects of the different types of spin-spin interactions on the nonzero temperature phase transition properties of the present system. Actually, such a binary alloy spherical nanoparticle can include four different values of spin-spin interaction terms between considered spins, that is to say, J_{AA} , J_{AB} , J_{BA} and J_{BB} corresponding to the randomly distributed components between $A - A$, $A - B$, $B - A$ and $B - B$, respectively. It is also possible to improve the obtained results in this study by making use of a more realistic system

such as classic Heisenberg type Hamiltonian where the spins are allowed to point in any direction. From theoretical perspective, this type of model containing the different types of spin-spin interactions mentioned above may be subject of a future work in order to provide deeper understanding of thermal and magnetic phase transition properties of the nanoparticle systems.

Acknowledgements

The numerical calculations reported in this paper were performed at TÜBİTAK ULAKBİM (Turkish agency), High Performance and Grid Computing Center (TRUBA Resources).

References

- [1] A.E. Berkowitz, R.H. Kodama, S.A. Makhlof, F.T. Parker, F.E. Spada, E.J. McNiff Jr., S. Foner, *J. Magn. Magn. Mat.* 196 (1999) 591.
- [2] M.L. Plumer, J. van Ek, D. Weller, *The Physics of Ultrahigh-Density Magnetic Recording*(Springer Series in Surface Sciences) 41 (2001).
- [3] T. Hayashi, S. Hirono, M. Tomita, S. Umemura, *Nature* 381 (1996) 772.
- [4] R.L. Comstock, *Introduction to Magnetism and Magnetic Recording*, Wiley, New York (1999).
- [5] Q.A. Pankhurst, J. Connolly, S.K. Jones, J. Dobson, *J. Phys. D: Appl. Phys.* 36 (2003) R167.
- [6] J. Rivas, M. Boñobre-López, Y. Piñero-Redondo, B. Rivas, M.A. López-Quintela, *J. Magn. Magn. Mater.* 324 (2012) 3499.
- [7] R.P. Blakemore, *Annu. Rev. Microbiol.* 36 (1982) 217.
- [8] D.A. Bazylinski, R.B. Frankel, H.W. Jannasch, *Nature* 334 (1988) 518.
- [9] Y.P. Ivanov, A. Alfadhel, M. Alnassar, J.E. Perez, M. Vazquez, A. Chuvilin, J. Kosel, *Sci. Rep.* 6 (2016) 24189.
- [10] P. Bhatt, A. Kumar, S.S. Meena, M.D. Mukadam, S.M. Yusuf, *Chem. Phys. Lett.* 651 (2016) 155.
- [11] V.S. Leite, W. Figueiredo, *Physica A* 350 (2005) 379.
- [12] T. Kaneyoshi, *J. Magn. Magn. Mater.* 321 (2009) 3430.
- [13] T. Kaneyoshi, *Physica Status Solidi B* 246 (2009) 2359.
- [14] D.A. Garanin, H. Kachkachi, *Phys. Rev. Lett.* 90 (2003) 065504.
- [15] H. Wang, Y. Zhou, D.L. Lin, C. Wang, *Physica Status Solidi B* 232 (2002) 254.
- [16] Y. Kocakaplan, M. Keskin, *J. Appl. Phys.* 116 (2014) 093904.
- [17] W. Jiang, X.-X. Li, L.-M. Liu, J.-N. Chen, F. Zhang, *J. Magn. Magn. Mater.* 353 (2014) 90.
- [18] T. Kaneyoshi, *J. Phys. Chem. Solids* 96-97 (2016) 1.
- [19] T. Kaneyoshi, *Solid State Commun.* 244 (2016) 51.
- [20] S. Bouhou, I. Essaoudi, A. Ainane, R. Ahuja, *Physica B* 481 (2016) 124.
- [21] E. Kantar, *J. Alloys Compd.* 676 (2016) 337.
- [22] M. El Hamri, S. Bouhou, I. Essaoudi, A. Ainane, R. Ahuja, *F. Dujardin, Appl. Phys. A* 122 (2016) 202.
- [23] H. Magoussi, A. Zaim, M. Kerouad, *Solid State Commun.* 200 (2014) 32.
- [24] G. Margaritis, K.N. Trohidou, J.J. Nogués, *Adv. Mater.* 24 (2012) 4331.
- [25] M. Vasilakaki, K. Trohidou, J. Nogués, *Sci. Rep.* 5 (2015) 9609.
- [26] L.B. Drissi, S. Zriouel, *J. Stat. Mech.* (2016) 053206.
- [27] A. Zaim, M. Kerouad, *Physica A* 389 (2010) 3435.
- [28] N. Zaim, A. Zaim, M. Kerouad, *J. Alloys Compd.* 663 (2016) 516.
- [29] N. Zaim, A. Zaim, M. Kerouad, *Solid State Commun.* 246 (2016) 23.
- [30] S. Aouini, S. Ziti, H. Labrim, L. Bahmad, *Solid State Commun.* 241 (2016) 14.
- [31] A. Feraoun, A. Zaim, M. Kerouad, *J. Phys. Chem. Solids* 96-97 (2016) 75.
- [32] W. Jiang, J.-Q. Huang, *Physica E* 78 (2016) 115.
- [33] V. Russier, *J. Magn. Magn. Mater.* 409 (2016) 50.
- [34] M.F. Thorpe, A.R. McGurn, *Phys. Rev. B* 20 (1979) 2142.
- [35] R.A. Tahir-Kheli, T. Kawasaki, *J. Phys. C* 10 (1977) 2207.
- [36] J.A. Plascak, *Physica A* 198 (1993) 655.
- [37] S. Katsura, F. Matsubara, *Can. J. Phys.* 52 (1974) 120.
- [38] R. Honmura, A.F. Khater, I.P. Fittipaldi, T. Kaneyoshi, *Solid State Commun.* 41 (1982) 385.
- [39] T. Kaneyoshi, *Phys. Rev. B* 34 (1986) 7866.
- [40] T. Kaneyoshi, *Phys. Rev. B* 33 (1986) 7688.
- [41] T. Kaneyoshi, Z.Y. Li, *Phys. Rev. B* 35 (1869).
- [42] T. Kaneyoshi, *Phys. Rev. B* 39 (1989) 12134.
- [43] P.D. Scholten, *Phys. Rev. B* 32 (1985) 345.
- [44] P.D. Scholten, *Phys. Rev. B* 40 (1989) 4981.
- [45] M. Godoy, W. Figueiredo, *Int. J. Mod. Phys. C* 20 (2009) 47.
- [46] D.S. Cambui, A.S. De Arruda, M. Godoy, *Int. J. Mod. Phys. C* 23 (2012) 1240015.
- [47] K. Binder, *Monte Carlo Methods in Statistical Physics* (Springer, Berlin, 1979).
- [48] M.E.J. Newman, G.T. Barkema, *Monte Carlo Methods in Statistical Physics* (Oxford University Press, New York, 1999).
- [49] Y. Yüksel, *Phys. Rev. E* 91 (2015) 032149.

- [50] L. YunBin, L. ShuZhi, X. Bin, C. Jia, P. HaoJun, Z. Chun, Z. HuiYing, X. HaoWen, O. YiFang, Z. BangWei, *Science China Physics, Mechanics and Astronomy*, 54 (2011) 897, and references therein.
- [51] E. Vatansever, H. Polat, *Phys. Lett. A* 379 (2015) 1568.
- [52] E. Vatansever, U. Akinci, H. Polat, *J. Magn. Magn. Mater.*, 389 (2015) 40.